

NTM induced fast ion losses in ASDEX Upgrade

This content has been downloaded from IOPscience. Please scroll down to see the full text.

2007 Nucl. Fusion 47 L10

(<http://iopscience.iop.org/0029-5515/47/7/L03>)

View [the table of contents for this issue](#), or go to the [journal homepage](#) for more

Download details:

IP Address: 200.0.233.52

This content was downloaded on 03/02/2014 at 20:09

Please note that [terms and conditions apply](#).

LETTER

NTM induced fast ion losses in ASDEX Upgrade

M. García-Muñoz¹, P. Martin^{2,3}, H.-U. Fahrbach¹, M. Gobbin^{2,3},
S. Günter¹, M. Maraschek¹, L. Marrelli², H. Zohm¹ and
the ASDEX Upgrade Team

¹ Max-Planck-Institut für Plasmaphysik, EURATOM Association, Boltzmannstr. 2, Garching D-85748, Germany

² Consorzio RFX, Associazione EURATOM-ENEA per la Fusione, Padova, Italy

³ Dipartimento di Fisica, Università di Padova, Padova, Italy

E-mail: Manuel.Garcia-Munoz@ipp.mpg.de

Received 19 December 2006, accepted for publication 2 May 2007

Published 13 June 2007

Online at stacks.iop.org/NF/47/L10

Abstract

The loss of fast (i.e. suprathermal) ions from a magnetically confined fusion plasma due to the interaction with magnetohydrodynamic (MHD) instabilities has been experimentally characterized and interpreted by means of a numerical model. It is found that for a special class of instabilities, the so-called neoclassical tearing modes, fast ion losses are increased and modulated at the same frequency of the mode. This new experimental finding is explained as a result of the drift islands formed by energetic ions in particle phase space. An eventual overlapping of these drift islands leads to an orbit stochasticity and therefore to an enhancement of the fast ion losses. This explanation is confirmed by statistical analysis of simulations of fast ions trajectories performed with the ORBIT code. The mechanism is of general importance for understanding the interaction between MHD modes and fast particles in magnetic confinement experiments.

PACS numbers: 52.35.Fi, 52.35.Py, 52.50.Gj, 52.55.Fq, 52.55.Pi, 52.55.Fa, 52.55.Dy, 52.65.Cc, 52.55.Tn

(Some figures in this article are in colour only in the electronic version)

A significant fraction of plasma pressure in a magnetized fusion experiment is carried by suprathermal (fast) ions, which are produced either by fusion reactions (like α particles), injected through energetic beams, or by RF heating. In general, these fast particles play an important role in the energy balance of a fusion plasma, either for heating and/or for current drive processes [1–3]. The confinement of fast particles is therefore an issue of great importance, since significant losses of these ions may drastically reduce the heating as well as the current drive efficiency. In addition, an intense and localized loss of fast ions may cause damage to plasma facing components. Due to their high energy, the dynamics of fast ions in a magnetized plasma is rather different from that of thermal ions and, in many aspects, still experimentally unexplored. Several issues are still open, for example, about the interplay between a population of fast particles and a key player of magnetized fusion plasmas, such as magnetohydrodynamic (MHD) instabilities.

In this letter we present the first measurements of fast ion losses (FIL) with simultaneous high time, energy and pitch angle resolution due to neoclassical tearing modes (NTMs). We explain the measurements on the basis of drift islands and their overlap, which leads to orbit stochasticity. The main experimental phenomenology is in fact reproduced by a model simulating the guiding centre orbits of fast ions. The results reported here are important for next-step fusion devices such as ITER where a significant population of α -particles and of NBI and ICRH generated fast ions will be present.

NTMs are metastable modes driven by the missing bootstrap current within a preexisting seed magnetic island, provided that the plasma poloidal beta, β_{pol} , is larger than the threshold value [4]. When a NTM grows in the plasma, global confinement is severely affected. NTMs set the limit to the maximum β_{pol} achievable in conventional scenarios. While the NTM impact on the global confinement is rather well established, less is known on how they influence energetic

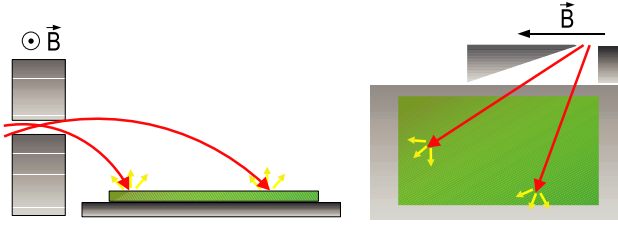


Figure 1. Schematic of the FILD principle. The probe consists basically of one aperture which disperses the NBI ion losses according to the gyroradius and the pitch angles onto the scintillator. Two different particle trajectories have been drawn, showing how the aperture works in the perpendicular and the parallel directions to the magnetic field.

particles, for example, ICRH heated ions or ions of neutral beam injection (NBI) origin. Experiments on this subject have been performed in TFTR [5, 6] and DIII-D [7]. The study of the effect of NTMs on the fast ion confinement is important, for example, to fully assess the efficiency of NBI heating and current drive. In next generation devices, such as ITER, this information is important also to predict the confinement of alpha particles and the impact of their losses on plasma facing components.

The ASDEX Upgrade (AUG) tokamak [8] has unique capabilities for fast particle studies: its heating system, with 20 MW of NBI at 60/93 keV, 6 MW of ICRH and 2 MW of ECRH, allows a rich variety of scenarios, where the behaviour of fast ion population can be finely tuned and decoupled from the bulk plasma environment. AUG is equipped with 8 NBI sources, each one capable of supplying 2.5 MW at different injection angles.

A new diagnostic in AUG, the fast ion loss detector (FILD), provides energy and pitch angle resolved measurements of FIL, with a bandwidth of 1 MHz [9]. Its design is based on the concept of the α -particle detector used for the first time at TFTR [10] and more recently at W7-AS [11]. The active part of the diagnostic is a scintillator plate contained within a cylindrical cup, which can be inserted via a movable manipulator up to a few mm behind the limiter slightly above the mid plane. Fast ions enter the detector through an aperture open in the cup and hit the scintillator. Their strike points depend on fast particles gyroradius (i.e. their energy) and on their pitch angle, defined as the angle between their velocity and the local magnetic field B , figure 1. The scintillating surface is observed via a CCD camera, which provides a slow but highly spatially resolved image, and by an array of 20 photomultipliers, which have a bandwidth of 1 MHz and provide therefore a very high time resolution.

The experiments discussed in this letter have been mainly performed in plasmas with a toroidal current of $I_p = 0.8$ MA, a toroidal field of $B_t = 2$ T, a safety factor at the edge of $q_{95} = 4.5$ and NBI as main heating and fast particle source. Time traces of the total NBI power and the magnetic fluctuations due to the $(m = 2, n = 1)$ and the $(m = 3, n = 2)$ NTMs for a typical discharge (#21089) are shown at the bottom of figure 2. An NBI power ramp in the period 1–2 s excites a $(2,1)$ NTM, which changes strongly in the frequency and resonance location during the NBI modulation phase 2–3 s. Between $t = 3$ s and $t = 5$ s the mode reaches a plateau phase in which it maintains constant its main features, i.e.

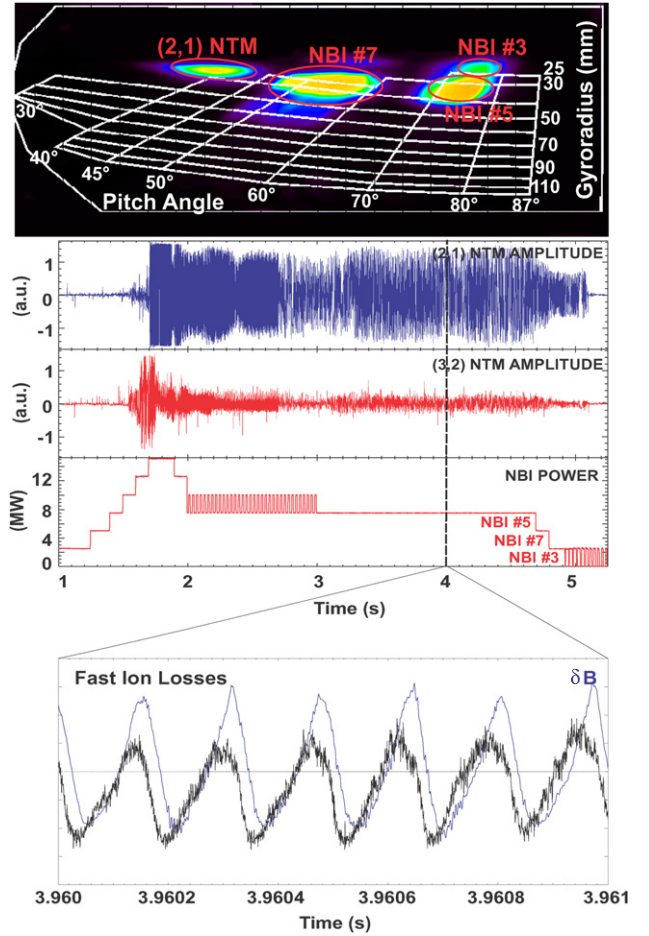


Figure 2. AUG discharge #21089. *Top frame:* CCD picture showing the three spots produced by first orbit losses from NBI sources #3, #5 and #7 and $(2,1)$ NTM induced FIL. *Mid frames:* global magnetic fluctuation amplitude $\delta B(t)$ for the modes with odd toroidal mode number (this signal is dominated by the contribution of the $(2,1)$ mode) and with even toroidal mode number (in this case the signal is dominated by the contribution of the $(3,2)$ mode); waveform of the total NBI power. *Bottom frame:* time evolution of the amplitude of a FIL signal (black curve) and of the magnetic fluctuation due to the $(2,1)$ mode (blue curve) in a short time window including a few mode oscillations.

frequency, resonance location and amplitude. This phase has been selected to study the properties of the $(2,1)$ NTM induced fast ion loss and its dependence on the mode amplitude.

In order to identify the lost particles in phase space we analyse the loss pattern recorded by the CCD camera during the MHD activity. On top, figure 2 shows a CCD frame for the discharge #21089 at $t = 4.03$ s, when the NTM is present; $(2,1)$ NTM induced fast ion losses (FIL) together with the prompt losses generated by three different NBI sources are visible. The more radially injected ions (sources #3 and #5) appear in the region of a higher pitch angle (70° – 75°), while a tangential source (#7) produces prompt losses in a lower pitch angle region (50° – 60°). The pitch angle is defined as $\arccos(v_{\parallel}/v_{\text{tot}})$. The $(2,1)$ NTM contribution to the fast ion loss pattern shows a pitch angle selective character with two main components. First, a loss of fast ions appears only when the $(2,1)$ NTM is present in the phase space region corresponding to low pitch angles (35° – 45°) and to the NBI main injection energy, as

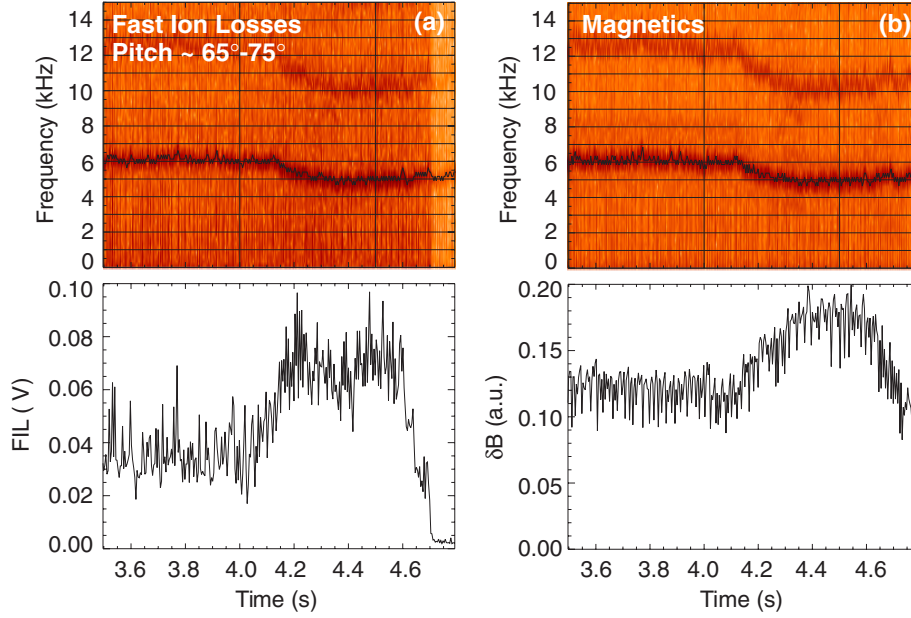


Figure 3. AUG discharge #21089. (a) *top*: spectrogram of the signal corresponding to FIL with pitch angle $\approx 65^\circ$ – 75° and gyroradii ≈ 40 mm; *bottom*: amplitude of FIL signal at the dominant frequency shown in the top frame. (b) *Top*: spectrogram of the magnetic fluctuation signal showing a dominant frequency (5–6 kHz) corresponding to a (2,1) NTM; *bottom*: amplitude of the magnetic fluctuation signal at the dominant frequency reported in the top frame.

reported in figure 2. In addition, when a (2,1) NTM is present, the prompt loss pattern due to NBI sources #5 and #7 shows a broader energy distribution which ranges from the injection energy, 93 keV (gyroradius of 40 mm) down to the minimal measurable energy, 60 keV (gyroradius of 25 mm). Figure 2 also shows the magnetic activity present in the discharge by means of the overall magnetic fluctuation signals due to modes with odd toroidal mode number (signal dominated by the (2,1) mode) and to modes with even toroidal mode number (signal dominated by the (3,2) mode). The waveform of the total NBI power is also shown. On the bottom, figure 2 shows one of the main findings of this work, i.e. the phase-locking between the (2,1) NTM magnetic fluctuation and the FIL during a time window of 10 ms. During this phase the experimental magnetic fluctuation level at the wall was $B_r(t) \approx 40$ mT.

To quantify the amount of lost particles due to the NTM magnetic perturbation and to separate these from the common NBI prompt losses, a fast fourier transformation (FFT) was applied to the signal of the photomultipliers which cover the phase space regions where NTM induced losses are observed, figure 3(a). The same FFT was also applied to the magnetic perturbation recorded by the Mirnov coils, figure 3(b). We observe a correlation between the frequency and the phase of the mode and those of the losses. Tracking the main frequency of magnetic perturbation and of the FIL we find, in general, a strong correlation between the NTM amplitude and the energetic particle loss signal.

The intermittent operation of NBI sources, with a switch-off time shorter than $50 \mu\text{s}$, has been used to provide a periodically changing source of fast particles which helps in the study of the loss time scales. In discharge #21168, NBI source #8 (which is injecting rather radially deuterium ions at 93 keV) has been modulated with square pulses of 2.5 MW amplitude, superimposed to a constant background of 5 MW.

In this discharge, a large (2,1) magnetic island is responsible for the FIL. A detailed analysis of the loss time scales reveals a different behaviour depending on the pitch angles of the lost ions. The losses of deuterons with energies $E \approx 93$ keV and rather parallel velocities (i.e. pitch angles $\approx 35^\circ$ – 45°), injected by the modulated beam, closely follow both the time evolution of their source and the mode evolution. Figure 4(a) shows the spectrogram of the FILD channel #7 corresponding to $E \approx 93$ keV and pitch angle $\approx 35^\circ$ – 45° . Besides the slow trend following the frequency evolution of the mode and of its harmonics, we note discrete spots corresponding to the NBI modulation. As shown in figure 4(b), the amplitude of the losses at the dominant mode frequency (black curve) is modulated according to the NBI evolution (red curve) and its envelope follows the amplitude of the magnetic mode (blue curve). Looking more closely into an individual NBI square pulse, figure 4(c), we observe that the losses recorded by the FILD channel #7 promptly decay as soon as the modulated source is switched off, thus indicating a time scale for these losses not larger than a few tens of μs . The FILD channel #9 (figure 4(d)), which corresponds to lost particles with $E \approx 93$ keV and pitch angles $\approx 70^\circ$ – 75° , shows different features. While the modulation pattern is still recognizable, after the beam switch-off there is a tail in the loss signal, corresponding to a time scale of the order of few ms for this kind of particles. Both signals show a strong correlation between the amount of FIL and the amplitude of the magnetic perturbation.

The absolute amount of lost ions has been estimated taking into account the photomultiplier signals and the number of photons produced by each incident ion in the scintillator plate (ionoluminescence). The scintillator ionoluminescence was calibrated in an accelerator facility [9]. The typical lost ion flux varies from $4 \times 10^{13} \text{ Ions s}^{-1} \text{ cm}^{-2}$ for the NTM prompt losses up to $10^{14} \text{ Ions s}^{-1} \text{ cm}^{-2}$ for the lost ions with higher

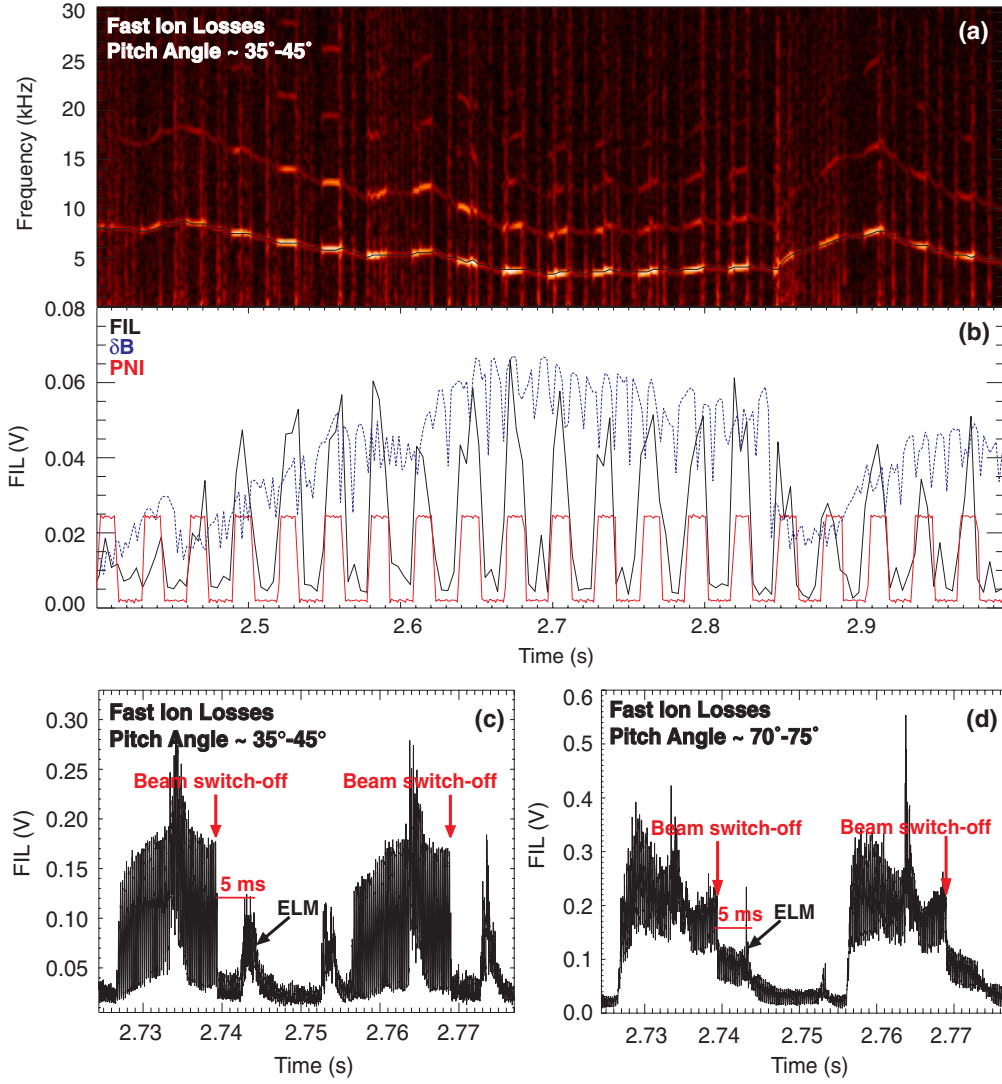


Figure 4. AUG discharge #21168: (a): spectrogram of the FILD signal corresponding to losses with pitch angle $\approx 35^\circ\text{--}45^\circ$. (b): waveforms of NBI modulated power (red curve; modulation amplitude 2.5 MW), of the amplitude of the (2,1) mode (blue dotted curve) and of the amplitude of the FILD signal in the top frame at the frequency of the (2,1) NTM (black curve). (c), (d): two FILD channels corresponding to two pitch angle regions, showing different temporal behaviors when the modulated beam is switched-off.

pitch angle. Both signals are of the same order as the maximal NBI prompt loss signal, 4×10^{14} Ions $\text{s}^{-1} \text{cm}^{-2}$. Comparing the NTM induced FIL with the NBI prompt losses and taking into account that the first ones should be toroidally distributed and the prompt losses are well localized, the importance of this study is made clear.

The experimental findings presented in this letter are discussed in the framework of a mechanism, which involves drift islands in the fast particle orbit space [12].

This mechanism is the result of the interaction of energetic ion motion with a magnetic equilibrium perturbed by a long-wavelength mode. A single helicity magnetic perturbation, such as that due to the (2,1) NTM, produces an island chain in the magnetic field. These magnetic islands do not cause significant ergodicity of magnetic field lines (followed by the guiding centres of thermal particles) for the amplitudes observed here. The situation for fast particles is different: the coupling between the fast particles guiding centre motion in the perturbed magnetic field and the orbit shift due to the drifts

(which has a $(m = 1, n = 0)$ character) results in several chains of drift islands (of (1,1), (2,1), (3,1) and (4,1) helicities) in fast particle phase space. Depending on the shape of the q -profile, on the location of the $q = 2$ resonance and on the amplitude of the original (2,1) mode, these islands may or may not overlap, but in both cases they may drive fast particle losses. If there is overlapping, a stochastic region is created in the fast particles orbit space, which leads to significant losses [12].

This problem has been studied by computing the trajectories of fast ions, injected by NBI in a tokamak magnetic equilibrium perturbed by a (2,1) mode. The simulation has been performed with the Hamiltonian guiding centre code ORBIT [13], which is that used in [5, 7]. For this study a circular cross section equilibrium has been considered: this choice strongly facilitates the problem from a numerical point of view, with the drawback that the comparison with the experiment cannot be pushed up to very quantitative levels.

The initial fast ion population has been chosen as that resulting by the ionization pattern of the applied NBI sources

in a plasma with the global parameters corresponding to those of the plasma in figure 3. The ionization pattern was calculated using the FAFNER code [14], which provides the birth location, energy and pitch angle of the injected NBI ions. The pitch angle of the ions at the starting point depends on the injection direction of the NBI source and the local magnetic field. The resulting distribution of about 90 000 ions with energies above 90 keV, originally produced for the D-shaped plasma, has been re-mapped into the circular equilibrium and has been taken as the initial particle distribution for ORBIT. A circular cross section tokamak equilibrium with the same AUG major radius, and a minor radius equal to the average between the two semi-axis of the AUG D-shaped cross section, a toroidal field $B_t = 2$ T and a superimposed stationary ($m = 2, n = 1$) perturbation has been considered. The perturbation for the (2,1) NTM implemented in the code is stationary and is given by $\delta \mathbf{b} = \nabla \times \alpha \mathbf{B}_0$ with the following expression for the eigenfunction α :

$$\alpha(\Psi_p, \zeta, \theta) = \alpha_0 r(\psi_p)^m (\psi_p - \psi_w) \sin(n\zeta - m\theta + \Phi),$$

where (m, n) is the helicity of the mode, $r(\psi_p)$ is the normalized radius as a function of the poloidal flux, ψ_w is the poloidal flux at the wall and Φ is the mode phase.

Its amplitude has been chosen to produce a magnetic island size consistent with experimental measurements, i.e. ≈ 10 – 12 cm in the low field side. Interactions of fast ions with the background plasma, i.e. pitch angle scattering and slowing down, have been included in the simulations. The trajectories of a set of test fast particles all starting at $t = 0$ are integrated over time and all the information about particles that reach the wall is recorded. The first evidence is that the presence of the mode causes a significant enhancement of the fraction of simulated fast particles reaching the wall, mostly concentrated in a toroidally localized region (which, as we will see in figure 6, it is a signature of the $n = 1$ character of the losses) and close to the equatorial mid-plane. With the mode eigenfunction used in this paper, an amount of losses of the order of 10% of the injected fast ion population is observed within a few ms. This number is only indicative, since the assumptions used in the model, and in particular the circular geometry instead of the D-shaped geometry, do not allow a precise quantitative estimate of the losses. The elongation of the flux surfaces could, for example, reduce the drift orbit displacement.

In figure 5 we show the distribution of the pitch of lost ions. For this figure, we have considered the particles lost within a limited region in toroidal and poloidal angles, where the effect of the mode is concentrated, see figure 6. All these particles have basically their birth energy, i.e. 93 keV. For comparison the distribution of the losses without the mode is also shown (red curve); the two peaks in the distribution without the mode correspond to first orbit losses for the two 93 keV beams used in this simulation. The increase in losses is different for particles of different pitches: in particular a large increase is observed around 45° . This peak has interesting analogies with the experimental observations. At this pitch angle, in fact, a spot is found in the CCD image (which is labelled (2,1) NTM in figure 2). The experimental losses corresponding to that spot appear only when the mode is present, a fact which is consistent

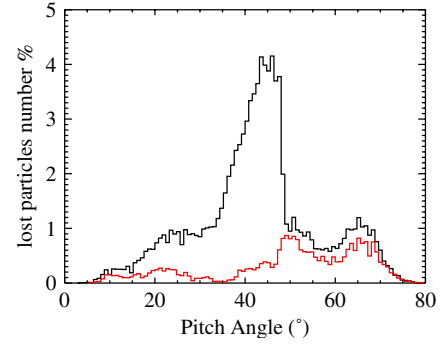


Figure 5. Histograms of the pitch angles of particles lost during the ORBIT simulation with perturbation (black line) and without it (red line).

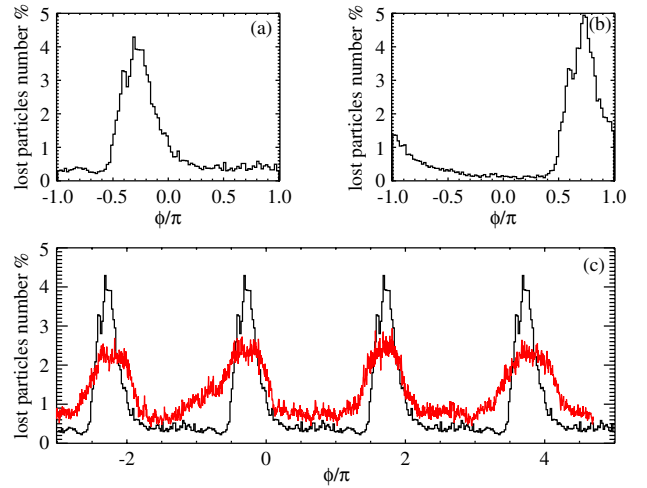


Figure 6. Toroidal angle distribution of simulated losses as a function of the toroidal angle, ϕ . The two panels (a) and (b) show histograms for two choices of the phases of the ($m = 2, n = 1$) mode, differing by π . In (c) a comparison between the simulation (black line) and the experimental data (red line) is shown.

with the prediction of the appearance of the peak in figure 5. A peak in the numerical losses is also observed around 70° , which is consistent with the corresponding experimental spot due to NBI source #3 (see figure 2). The increase in losses in the simulation due to the mode is much smaller than that for the pitch region around 45° . This might be due to the fact that these particles are trapped, and in the numerical simulation magnetic ripple and mode rotation have not been included. The peak around 50° – 55° corresponding to NBI source #7 is not evident in the simulation, though losses increase slightly in that region. Likely we have a merging with the adjacent peak, possibly due to the limits of the model. Moreover, for computational reasons, statistically significant results are obtained integrating losses over a range of toroidal angles, while the measurement is toroidally localized. It is worth noting that the simulation also shows losses at pitch angles $< 35^\circ$, which cannot be detected by the FILD.

In order to compare the simulation results with the FILD time traces, the distribution of the toroidal loss angles for particles with a pitch $\approx 45^\circ$ (corresponding to the peak of losses in the presence of the NTM) is shown in figure 6(a): it is

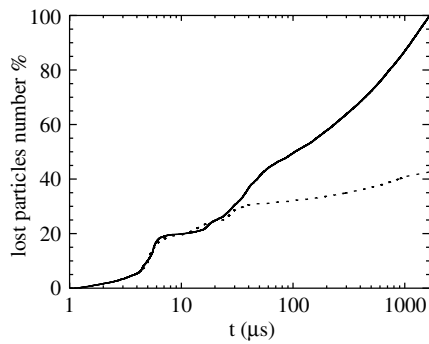


Figure 7. Integral probability distribution of the loss times of fast particles with energy $E > 90$ keV in the presence of the perturbation (solid line) and without it (dashed line). Both curves are normalized to the number of $E > 90$ keV particles lost in the simulation with an NTM.

characterized by a single peak, reflecting the $n = 1$ nature of the losses. The location of the peak is correlated with the phase of the magnetic perturbation: figure 6(b) shows the histogram of the losses for a simulation where the phase of the ($m = 2, n = 1$) perturbation was displaced by π . This is in agreement with the experimentally observed modulation of the losses at the frequency of the NTM (figure 3). Moreover, a direct comparison with experimental data can be done by reporting them on the toroidal distribution of the simulated losses. The result is shown in figure 6(c) where a few periods of the FILD signal have been superimposed on the simulated toroidal distribution (replicated several times) by mapping time into the toroidal angle, assuming a rotation with constant angular velocity and adjusting the initial phase to match the maximum. The amplitude of the signal is multiplied only by a constant without any change in the offset. The agreement with the experiment is qualitatively good. Finally we considered the distribution of the times at which simulated particles were lost. The integral probability distribution of loss times for the lost particles described in figure 5 is reported in figure 7, for the case with NTM (solid curve) and without (dashed curve). For a given value in the x -axis, the curve provides the number of lost particles, which leave the plasma within that time. The plot shows that particles are lost in a broad range of time scales: while the first are promptly lost after $\approx 10 \mu\text{s}$ (to be compared with the toroidal transit time for 100 keV deuterons equal to $5 \mu\text{s}$) a fraction of the population takes a longer time before escaping. This

phenomenology is similar to the experimental observation of ions being lost on a slow time scale (figure 4, lower right frame). In fact, the particles with the shortest loss times are those deposited by the NBI system on the high field side well inside the separatrix and cross readily onto the low field side due to the torus drift displacement of their orbits. The modulation with the island frequency can be explained by the drift islands with (3,1) and (4,1) helicities. Particle losses after longer times (hundreds of μs to ms time scale) are those more influenced by the stochastic diffusion. The comparison between the model and the experiment as far as loss times are concerned needs anyway to be considered as qualitative, because of the before mentioned limits of the numerical simulation.

In conclusion, the losses of fast ions driven by NTMs have been investigated in a variety of plasmas produced in AUG. The experimental data indicate that NTMs and in general magnetic islands produced by slow MHD modes are responsible for an important enhancement of the outward radial transport of NBI generated fast ions. A mechanism, based on the drift islands in the particle phase space, has been identified as the process responsible for these losses being the numerical predictions consistent with experimental data.

The authors wish to acknowledge the valuable support of V. Igochine, P. Piovesan, M. Reich, A. Stabler, E. Strumberger and R. B. White (Princeton Plasma Physics Laboratory, PPPL).

References

- [1] Heidbrink W.W. *et al* 1994 *Nucl. Fusion* **34** 535
- [2] Sharapov S.E. *et al* 2000 *Nucl. Fusion* **40** 1363
- [3] Pinches S.D. 2004 *Plasma Phys. Control. Fusion* **46** B187
- [4] Chang Z. *et al* 1995 *Phys. Rev. Lett.* **74** 4663
- [5] Zweben S.J. *et al* 1999 *Nucl. Fusion* **39** 1097
- [6] Zweben S.J. *et al* 2000 *Nucl. Fusion* **40** 91
- [7] Carolipio E.M. *et al* 2002 *Nucl. Fusion* **42** 853
- [8] Herrmann A. 2003 *Fusion Sci. Technol.* **44** 569
- [9] Garca-Muoz M. 2006 Fast response scintillator based detector for MHD induced energetic ion losses in ASDEX Upgrade *PhD Thesis* Ludwig-Maximillan-University of Munich
- [10] Darrow D.S. 1995 *Rev. Sci. Instrum.* **66** 476
- [11] Werner A. and Weller A. 2001 *Rev. Sci. Instrum.* **72** 780
- [12] Mynick H.E. 1993 *Phys. Fluids B* **5** 1471
- [13] White R.B. 1984 *Phys. Fluids* **27** 2455
- [14] Lister G.G. 1985 A fully 3-d neutral beam injection code using monte carlo methods *Technical Report* IPP 4/222 Max-Planck-Institut fuer Plasmaphysik